

Effect of pulsed laser damage on the thermal properties of metal film on substrate

T. A. El-Dessouky¹, Y. A. Badr², S. E.–S. Abd El-Ghany³, A. E.–S. B. Ammar³

¹(Faculty of Science, Ain Shams University, Cairo, Egypt)

²(National Institute of Laser Enhanced Sciences (NILES), Cairo University, Giza, Egypt)

³(Faculty of Science, Benha University, Benha, Egypt)

Corresponding Author: T. A. El-Dessouky

Abstract: Two thin films of antimony and copper were coated on stainless steel substrate. The thicknesses of the films were 130 nm and 150 nm for antimony and copper respectively which measured interferometrically. The resultant damage in the targets depends on the total thermal properties of thin films as well as their reflectivities. Good conductor films distribute the incident heat horizontally more than in vertical direction. Meanwhile, bad conductor films confine the incident energy in the vertical direction rather than the horizontal. Also most of the incident energy was found to be used for evaporation of the particles of the good conductor.

Keywords: Laser damage, thermal diffusion, evaporated materials, residual material, Kinetic energy.

Date of Submission: 04-02-2019

Date of acceptance: 22-02-2019

I. Introduction

Laser damage in metallic thin films has many applications. It plays a principle role in production of electronic circuits and devices [1,2], manufacturing solar cells [3-5], patterning thin metal film [6] and generation of nano-particles [7]. As well as fabrication of contact masks elements of diffractive optics [8], optical gates [9,10], modification of electrical properties and surface morphology [11], ...etc. Many studies investigated the effect of laser's parameters and material's properties on the damage process. The laser damage in a target coated with double metallic layers was four times greater than damage when the same target coated with single layer at the same thickness and laser power [12]. The damage process in thin film of beam splitters was studied [13]. The film was irradiated with the wavelengths 1064 nm and 532 nm separately and with the both wavelengths simultaneously. It was found that, the damage induced by submicron-defects between the film and splitter. The effect of effective penetration depth on the glass substrate coated with 430 nm molybdenum thin film was studied [14]. A high efficient confined ablation was observed when effective penetration depth was lower than the thickness of the film.

Also, the effect of material's properties was studied. The threshold energies irradiated thin metal films of nickel (100 nm), gold (350 nm) and copper (360 nm) were given by 8.26 μJ, 10.82 μJ and 13.25 μJ for 360 nm copper respectively where nanosecond pulsed Nd:YAG laser at 355 nm was used [15]. The Micro-scribing of copper/ aluminum films irradiated with 1064 nm, 532 nm and 355 nm in air and water media were examined [16]. In water medium, the ablation of aluminum film was more effective when the shorter wavelengths were used, whereas longer wavelengths ablated more for copper film. Also, there was not any debris around damage in water medium. The fluences between 0.7 - 1.1 J/cm² were suitable for patterning chromium film with thickness 100 nm coated on glass substrate [17].

Theoretical model was used to predict the temperature distributions in molten layer of thin film on substrate, solid part of thin film and in substrate using Laplace transform technique during irradiation with pulsed laser [18]. The Laplace transform technique was used to obtain a formula for time dependence of both the evaporation part and the molten layer thickness of thin film [19]. Also, the temperature-dependent absorption coefficient of thin film was taken into account. Another theoretical analysis was used to solve the problem of melting and evaporation of both a semi-infinite and finite targets induced by surface absorption of a laser pulse [20-25].

The aim of this work is to investigate the effect of thermal properties of copper "Cu" and antimony "Sb" thin films coated on stainless steel substrate, on the damage process. Such investigation needs more studies and that is our interest for this work.

II. Experimental work

Two thin metal films of copper and antimony were thermally deposited separately on a commercial stainless-steel-430 substrate. The thickness of copper and antimony were 150 nm and 130 nm respectively. The

thicknesses of the films were determined by Fizeau interferometry system. The films were irradiated with nanosecond Nd:YAG pulsed laser at wavelength 532 nm (second harmonic generation) using KDP crystal . The duration of the pulse was 6 ns at FWHM with repetition rate 1 Hz. The laser beam was collected with a lens of focal length 200 mm. The targets were placed at a distance 30 mm before focal spot of the lens to avoid air discharge. The laser beam was directed approximately normally to the targets. Once for each damage the calculated diameter of laser beam on the surface of the targets was 0.9 mm according to the technical report [26]. The average energy of the pulses is 35 ± 0.5 mJ. Considering the laser pulse is a Gaussian shape for the incident mode TEM₀₁.

The absorbed energy E_a on the surface of the target depends on the reflectivity according to “equation 1” [27];

$$E_a = E_f (1 - R) \quad (1)$$

where E_f is incident energy and R is reflectivity of material surface.

The thickness of films and the morphology of the surface of the targets were investigated by optical microscope and white light interference microscope (zygo).

III. Results and discussion

Figs. 1-2 show the morphology of the craters in Sb and Cu samples obtained by optical microscope and zygo. From Fig. 2a the resultant depth was approximately 1 μ m. it means that the Sb layer was completely removed. In addition to, the stainless steel's depth was approximately 0.77 μ m. meanwhile, from Fig. 2b for Cu layer the resultant damage was with in the depth of film thickness only.

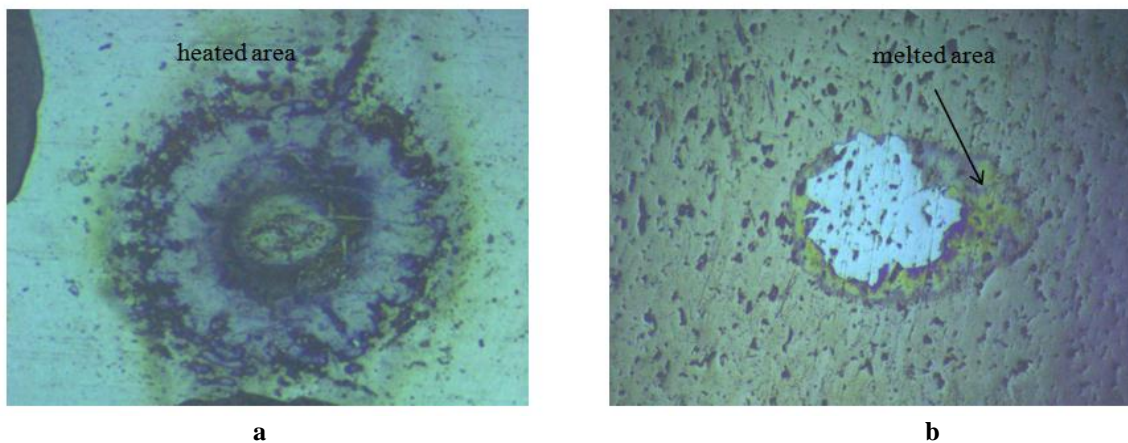


Fig. 1 shows morphology of the crater by optical microscope. (a) Sb/stainless steel target at 35.96 mJ. (b) Cu/stainless steel target at 34.52 mJ. (magnification 160x)

In the case of Sb/ stainless steel, burrs and sputtered of melting are formed around the entrance of the craters. The burrs were formed due to solidification of extracted melted materials from the craters as shown in fig. (2). Whereas in the case of Cu/stainless steel there is no burrs and sputtered melting around the craters.

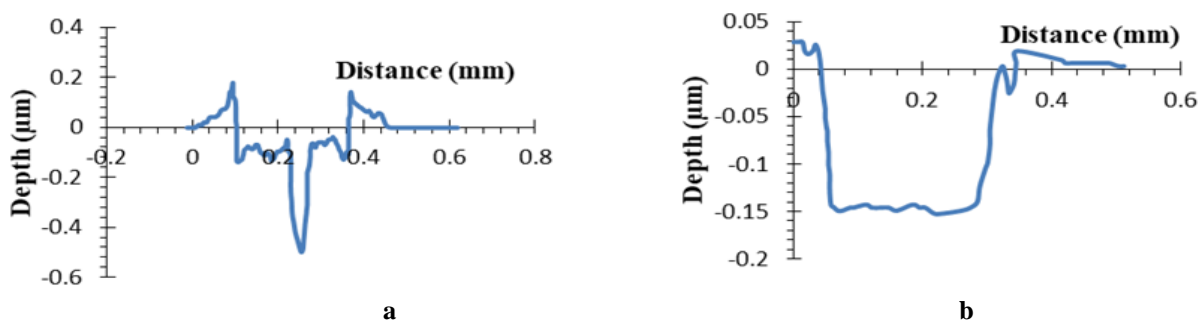


Fig. 2 shows damage in targets by Zygo microscope (a)Sb film of thickness 130 nm on stainless steel at 34.52 mJ. (b) Cu film of thickness 150 nm on stainless steel at 35.96 mJ.

The average diameter of craters for both, Sb and Cu targets were 0.5 mm and 0.4 mm respectively. The average ratios between the area of crater to the area of heat diffusion/melted area around the crater were 0.7 and 0.9 for Sb and Cu respectively.

The thermal diffusion length L_d of the target has an important role in illustrating the total removed part of Sb and Cu layers as given by “equation 2” [15];

$$L_d = \sqrt{4K\tau} \quad (2)$$

where $K=\alpha/(\rho C_p)$ is the thermal diffusivity, τ is pulse duration, α is thermal conductivity, ρ is density and C_p is specific heat of the target.

The calculated thermal diffusion lengths L_d of Sb and Cu using “equation 2” were 0.65 μm and 1.67 μm respectively. Because of the thickness of the films of Sb and Cu are smaller than the thermal diffusion lengths, they were completely removed. The thermal diffusion length L_d of Cu is nearly 3 times greater than Sb. The resultant damage not only interpreted on the base of thermal diffusion length L_d , but also on the other thermal properties of the films such as melting point, boiling point and latent heat. In general, the melting point, boiling point and latent heat of fusion are twice for Cu than Sb. Meanwhile, the latent heat of evaporation of Cu is 9 times of Sb [28]. So, we can explain the damage process not only to the thermal diffusion length L_d but also to other all thermal parameters. From Table 1, it was observed that the depth in stainless steel was slightly decreased, while the diameter of craters increased as the incident energy increased.

Table 1 shows the depth and diameter of damage in stainless steel substrate of Sb/ stainless steel target.

Incident energy (mJ)	Steel's depth (μm)	Steel's diameter (mm)
34.52	0.88	0.097
34.79	0.78	0.099
35.42	0.7	0.153
35.96	0.7	0.164

Therefore, assuming that the Sb layer of low thermal properties confined the spreading of heat in vertical direction rather than in horizontal direction. In the case of Cu i.e good conductor, the spreading of the heat will be more horizontally rather than the vertical direction. The same results were obtained for stainless steel which is a good conductor alloy.

The energy consumed to form the craters can be calculated using a simple model based on an energy conservation law of the following form [29];

$$E_c = m[C_p(T_v - T_o) + \Delta H_m + \Delta H_v], \quad (3)$$

where E_c is absorbed energy, m is removed mass, C_p is specific heat, T_v is boiling point, T_o is room temperature, ΔH_m and ΔH_v are latent heat of fusion and evaporation respectively of the target.

Table 2 shows the calculated absorbed energy E_c by using “equation 3” and actual absorbed energy E_a calculated by using “equation 1”. Assuming that the reflectivity of the materials is temperature independent and the reflectivity of Sb is 0.72 [30] and for Cu is 0.48 [31].

Table 2 shows actual absorbed energy from laser beam and calculated absorbed energies to form the craters in Sb and Cu targets.

Actual absorbed energy E_a (J)		Calculated energy in Sb and stainless steel E_c (J)		Total calculated energy in Sb/ stainless steel target (J)	Calculated energy in Cu/ stainless steel target E_c (J)
Sb	Cu	Sb	stainless steel		
9.66×10^{-3}	1.79×10^{-2}	2.46×10^{-4}	6.59×10^{-3}	6.84×10^{-3}	5.9×10^{-4}
9.74×10^{-3}	1.81×10^{-2}	2.54×10^{-4}	5.29×10^{-3}	5.55×10^{-3}	10^{-3}
9.92×10^{-3}	1.84×10^{-2}	2.60×10^{-4}	6.57×10^{-3}	6.83×10^{-3}	6.97×10^{-4}
1.01×10^{-2}	1.87×10^{-2}	2.89×10^{-4}	7.02×10^{-3}	7.31×10^{-3}	-

According to Table 2, it was found that the ratio between the calculated absorbed energy from “equation 3” to absorbed energy from “equation 1” equal to 70% for Sb target and 4% for Cu target. This difference is assumed as a kinetic energy of the evaporated particles.

Considering the evaporated mass and Avogadro's number of the used elements, the average velocity calculated for the evaporated particles of Cu which was approximately 11 km/sec. Meanwhile the average velocity for evaporated particles of Sb and stainless steel was approximately 2 km/sec.

According to the theory of the kinetic energy, the kinetic energy of the evaporated particles of Cu was about 25 times the kinetic energy of evaporated particles of Sb and stainless steel. The resultant high kinetic energy of Cu particles explains that most absorbed energy is used in totally evaporation without burrs at the edges of the craters and vice versa for Sb/stainless steel target.

From the resultant calculated velocities the time of evaporation from the craters was about 0.4 ns for antimony target. The evaporation time of copper particles was about 13 ps. Both times of evaporation in Sb and Cu targets were less than incident laser pulse duration which was 6 ns.

IV. Conclusion

From the previous work the following conclusions can be obtained:

- 1) The heat propagation of the incident laser beam on Cu and Sb coated films on stainless steel substrate depends on all thermal properties of the targets.
- 2) Substrate coated by film of low thermal properties such as Sb confines the heat in vertical direction rather than horizontal direction. On the other hand, a good conductor film like Cu film on stainless steel substrate distributes heat in horizontal direction rather than vertical direction.
- 3) The time of evaporated particles from the craters was inversely proportional to the thermal properties of the targets and directly proportional to their depths.

References

- [1]. Nicola Bellini, Riccardo Geremia, Shane Norval, Guillaume Fichet and DimirtrisKarmakis, Laser thin film patterning for rapid prototyping and customized production of flexible electronics devices, *Journal of laser micro/Nano engineering*, 11(3), 2016, 388-394.
- [2]. Dongkyoung Lee, Experimental investigation of laser ablation characteristics on nickel-coated beryllium copper, *Metals*, 8(4), 2018, 211.
- [3]. Charles A. Rohde, Hayley Ware, Fraser MacMillan, MalkhazMeladze and M. Cather Simpson, Selective gold film removal from multi-layer substrates with Nano-second UV pulsed ablation, *Appl. Phys. A*, 111, 2013, 531-537.
- [4]. Jim Bovatsek, AshwiniTamhankar, Raj Patel, Nadezhda M. Bulgakova and JörnBonse, Effects of pulsed duration on the ns-laser pulse induced removal of thin film materials used photovoltaic, *Society of photo-optical instrumentation engineers* 7201-41, (2009).
- [5]. J. Hermann, M. Benfarah, S. Bruneau, E. Axente, G. Coustillier, T. Itina, J-F. Guillemoles and P. Alloncle, Comparative investigation of solar cell thin film processing using nanosecond and femtosecond lasers, *Journal of physics D: Applied physics*, 39, 2006, 453-460.
- [6]. Philip D. Rack, Yingfeng Guan, Jason D. Fowlkes, Anatoli V. Melechko and Michael L. Simpson, Pulsed laser dewetting of patterned thin metal films; A means of directed assembly, *Applied Physics letters*, 92, 2008, 223108.
- [7]. R.G. Nikov, N. N. Nedyalkov, P. A. Atanasov and D. B. Karashanova, Synthesis of bimetallic nanostructures by nanosecond laser ablation of multicomponent thin films in water, *Journal of physics: series 992Conf.*, 2018, 012046.
- [8]. Poletaev S. D., Laser ablation of thin films of molybdenum for the fabrication of contact masks elements of diffraction optics with high resolution, *Information technology and nanotechnology CEUR workshop proceedings*, 1490, 2015, 82-89.
- [9]. V. S. Zuev and Yu. V. Senatsky, On the operation of optical shutter based on a thin metal film, *KratkieSoobshCheniya Po Fizike*, 42(4), 2015, 16-24.
- [10]. N. E. Bykovsky, S. M. Pershin, A. A. Samokhin and Yu. V. Senatsky, Transmittance jump in a thin aluminum layer during laser ablation, *Quantum electronics*, 46(2), 2016, 128-132.
- [11]. BibiZulaikaBhari, Ahmed Hadi Ali, AliyuKabiruIsiyaku and RabiatulAdawiah Ahmed, Comparative study of infrared Nd:YAG pulsed laser radiation on Pt thin film, *Journal of science and technology*, 9(3), 2017, 83-86.
- [12]. T. El Dessouki, I. Fouda, F. Sharaf and N. Khalil, Laser damage to metallic targets of different thermal properties, *Arab Gulf J. Scient. Ref.*, 3(1), 1985, 295-305.
- [13]. Lei Yan, Chaoyang Wei, Dawei Li, Kui Yi and Zhengxiu Fan, Dual-wavelength investigation of laser induced damage in multilayer mirrors at 532 and 1064 nm, *Optics communications*, 285, 2012, 2889-2896.
- [14]. Matthias Domke, Luigi Nobile, Stephan Rapp, SasiaEiselen, JürgenSotrop, Heinz P. Huber and Michael Schmidt, Understanding thin film laser ablation: the role of the effective penetration depth and the film thickness, *Physics procedia*, 56, 2014, 1007-1014.
- [15]. IstvánBozsóki, BálintBalogh and Péter Gordon, 355 nm nanosecond pulsed Nd:YAG laser profile measurement, metal thin film ablation and thermal simulation, *Optics and laser technology*, 43, 2011, 1212-1218.
- [16]. SrinagalakshmiNammi, Nilesh J. Vasa, Balaganesan G. and Anil C. Mathur, Pulsed laser assisted micro-scribing of metal thin films in air and under water using UV, visible and near IR wavelengths, *Procedia manufacturing*, 5, 2006, 684-695.
- [17]. S. K. Lee and S. J. Na, KrFexcimer laser ablation of thin Cr film on glass substrate, *Applied Physics A*, 68, 1999, 417-423.
- [18]. S. E. -S. Abd El-Ghany, The temperature profile in the molten layer of a thin-film coated on a substrate induced by irradiation with a pulsed laser, *Optics and laser technology*, 39, 2004, 95-106.
- [19]. S. E. -S. Abd El-Ghany and A. F. Hassan, Evaporation of a thin film coated on a substrate induced by a pulsed laser, *Optics and laser technology*, 39, 2007, 626-637.
- [20]. M. M. El-Nicklawy, A. F. Hassan, S. E.-S Abd El-Ghany, on melting a semi-infinite target using a pulsed laser, *Optics and laser technology*, 32, 2000, 157-164.
- [21]. S. E.-S Abd El-Ghany, the temperature profile in the molten layer of a semi-infinite target induced by irradiation using a pulsed laser, *Optics and laser technology*, 33, 2001, 539-551.
- [22]. S. E.-S Abd El-Ghany, on the evaporation of a semi-infinite target induced by a pulsed laser, *Optics and laser technology*, 36, 2006, 77-86.
- [23]. S. E.-S Abd El-Ghany, A theoretical study on the melting of a finite slab with a pulsed laser, *Optik*, 120, 2009, 890-897.
- [24]. S. E.-S Abd El-Ghany, A theoretical study on the evaporation induced by a pulsed laser in a finite slab, *Optics communications*, 282, 2009, 284-290.
- [25]. S. E.-S Abd El-Ghany, study the effect of spatial and temporal laser pulse profile on the heating a semi-infinite target in spherical coordinates, *International J. of Scientific & Engineering Research*, 6(4), 2015, 1391-1403.
- [26]. Chad Nelson, Jordan Crist, Predicting laser beam characteristics mode quality (M^2) measurement improves laser performance, *Wiley-VCH verlaggmbh&Co. Kga, Weinheim*, 1, 2012, 36-39.
- [27]. J. Wilson, J. F. B. Hawkes, *Laser principles and applications* (Europe, Prentice Hall, 1987).
- [28]. D.R. Lide, *HPRFrederikse .Handbook of chemistry and physics* (CRC press, Boca Raton, FL, 79, 1995).
- [29]. Karl-Heinz Leitz, Benjamin Redlingshöfer, Yvonne Reg, Andreas Otto and Michael Schmidt, Metal ablation with short and ultrashort laser pulses, *Physics procedia*, 12, 2011, 230-238.
- [30]. N. Srimathy, A. Ruban Kumar, Structural and optical characterization of thermally evaporated bismuth and antimony films for photovoltaic applications, *Science direct, Elsevier*, 39, 2016, 1-10.
- [31]. E. Hecht, *Optics* (England, Pearson Education Limited, 2017).